PHILOSOPHICAL TRANSACTIONS B

royalsocietypublishing.org/journal/rstb

Research

Cite this article: Fears KP *et al*. 2019 Adhesion of acorn barnacles on surface-active borate glasses. *Phil. Trans. R. Soc. B* **374**: 20190203.
http://dx.doi.org/10.1098/rstb.2019.0203

Accepted: 6 June 2019

One contribution of 15 to a theme issue 'Transdisciplinary approaches to the study of adhesion and adhesives in biological systems'.

Subject Areas:
biomaterials, bioinformatics, biomechanics

Keywords:
surface-active glass, aluminoborate glass, barnacle adhesion, *Amphibalanus amphitrite*, *Amphibalanus trigonus*

Author for correspondence:
Kenan P. Fears
e-mail: kenan.fears@nrl.navy.mil

Electronic supplementary material is available online at https://dx.doi.org/10.6084/m9.figshare.c.4587248.

THE ROYAL SOCIETY PUBLISHING

Adhesion of acorn barnacles on surface-active borate glasses

Kenan P. Fears[1], Andrew Barnikel[1], Ann Wassick[3], Heonjune Ryou[1], Janna N. Schultzhaus[2], Beatriz Orihuela[4], Jenifer M. Scancella[1], Christopher R. So[1], Kelli Z. Hunsucker[3], Dagmar H. Leary[2], Geoffrey Swain[3], Daniel Rittschof[4], Christopher M. Spillmann[2] and Kathryn J. Wahl[1]

[1]Chemistry Division, and [2]Center for Bio/Molecular Science and Engineering, US Naval Research Laboratory, 4555 Overlook Avenue SW, Washington, DC 20375, USA
[3]Center for Corrosion and Biofouling Control, Florida Institute of Technology, 150 West University Boulevard, Melbourne, FL 32901, USA
[4]Duke University Marine Laboratory, 135 Duke Marine Laboratory Road, Beaufort, NC 28516, USA

KPF, 0000-0002-3980-5266

Concerns about the bioaccumulation of toxic antifouling compounds have necessitated the search for alternative strategies to combat marine biofouling. Because many biologically essential minerals have deleterious effects on organisms at high concentration, one approach to preventing the settlement of marine foulers is increasing the local concentration of ions that are naturally present in seawater. Here, we used surface-active borate glasses as a platform to directly deliver ions (Na^+, Mg^{2+} and BO_4^{3-}) to the adhesive interface under acorn barnacles (*Amphibalanus* (=*Balanus*) *amphitrite*). Additionally, surface-active glasses formed reaction layers at the glass–water interface, presenting another challenge to fouling organisms. Proteomics analysis showed that cement deposited on the gelatinous reaction layers is more soluble than cement deposited on insoluble glasses, indicating the reaction layer and/or released ions disrupted adhesion processes. Laboratory experiments showed that the majority (greater than 79%) of adult barnacles re-attached to silica-free borate glasses for 14 days could be released and, more importantly, barnacle larvae did not settle on the glasses. The formation of microbial biofilms in field tests diminished the performance of the materials. While periodic water jetting (120 psi) did not prevent the formation of biofilms, weekly cleaning did dramatically reduce macrofouling on magnesium aluminoborate glass to levels below a commercial foul-release coating.

This article is part of the theme issue 'Transdisciplinary approaches to the study of adhesion and adhesives in biological systems'.

1. Introduction

Acorn barnacles inhabit marine environments across the globe. Once barnacle cyprids (last larvae stage) find suitable locations to settle, cyprids secrete proteinaceous cement and permanently attach themselves to surfaces where they subsequently undergo metamorphosis into sessile barnacles. Juvenile and adult barnacles periodically secrete concentric rings of cement [1], which mainly consist of insoluble protein nanofibrils [2]. Vibrational spectroscopy has revealed that barnacle cement, as a whole, has a high β-sheet content and spectral signatures characteristic of biogenic amyloid fibrils [3]. Barnacle cement reportedly consists of five major cement proteins (CPs, where the number corresponds to molecular weight in kDa), CP100, CP43 (=CP68), CP52, CP20 and CP19 [4–9]. We note that molecular weight of the full transcript of CP43 is 43 kDa, but its apparent molecular weight based on gel electrophoresis is approximately 68 kDa and its amino acid profile is consistent with the unsequenced CP68 from *Megabalanus rosa* [9]. While some CPs self-assembled

© 2019 The Author(s) Published by the Royal Society. All rights reserved.

into fibrils during *in vitro* experiments [10–12], the exact mechanisms of fibril formation and surface adhesion are unclear. Moreover, the identification of families of homologous CPs within cement plaques suggest that processes associated with barnacle adhesion are highly complex [9,13], as conserved domains within the CP19 family are amyloidogenic [14].

Through the use of *in situ* microscopy and spectroscopy, we have drawn a clear link between cement deposition and the moulting cycle of *Amphibalanus* (=*Balanus*) *amphitrite* [15–17]. Burden *et al*. [15] reported a correlation between the adhesion strength of re-attached barnacles and the completion of a moult cycle. Fears *et al*. [17] observed that epithelial cells, which form the basal cuticle, secrete cement fibrils through newly formed cuticle after the old cuticle moults and the barnacle enters the expansion phase. Unlike moulting processes in other crustaceans and insects, expansion of the barnacle base proceeds during moulting without the casting off of cuticle [16,17]. So *et al*. [9] extracted proteins from cement fibrils deposited on various substrates with hexafluoroisopropanol (HFIP) and found that AaCP43 (*A. amphitrite* cement protein) and AaCP19 are the predominant proteins while AaCP52 and AaCP100 were minor components.

In addition to the reputed structural CPs, multiple active enzymes, including proteases and cross-linkers (e.g. lysyl oxidase and transglutaminase), are present at the adhesive interface [9,18,19]. However, cuticular development, cement deposition and biomineralization all occur at this interface, so the identified enzymes could have functions other than cement curing. HFIP rinses efficiently liberated proteins in cement fibrils attached to borosilicate glass beads [9], indicating that the cement is not extensively cross-linked via covalent bonds. Sever *et al*. [20] and Zhao *et al*. [21] demonstrated that metal ions play a vital role in the curing of mussel and sandcastle worm adhesives, respectively. Unlike these other marine adhesives, adult barnacle cement does not contain 3,4-dihydroxyphenyl-L-alanine (DOPA) or phosphoserine [4,5,17,19], but cement curing could be mediated by the coordination of metal ions with acidic amino acids and the generation of reactive oxygen species. Therefore, manipulating the ion composition at the adhesive interface could affect the ability of barnacles to adhere.

Previously, we demonstrated that aluminoborate surface-active glasses are capable of preventing re-attached adult barnacles from permanently adhering to the glass surface [22]. By design, the glass networks of surface-active glasses readily hydrolyze in aqueous environments, releasing ions and metal oxides/hydroxides. Depending on the solubility of the released species and their reactivity with other ions at the interface, reaction layers immediately form on the glass surface as the glass network degrades [22–24]. In the case of aluminoborate glasses, gelatinous $Al(OH)_3$ layers form at the glass–water interface because $Al(OH)_3$ is the most thermodynamically favourable aluminium-containing phase ($K_{sp} = 4.6 \times 10^{-33}$) in seawater [22]. The local pH also increases during glass dissolution owing to the consumption of H^+ ions [25]. Therefore, the fouling-release behaviour of surface-active glasses could be owing to the local chemical environment and/or the properties of the gelatinous reaction layer.

Here, we elucidate the role of released ions and the reaction layer on the foul-releasing and antifouling performance of alkali and alkaline earth aluminoborate glasses ($2XO{\cdot}2Al_2O_3{\cdot}6B_2O_3$; denoted 2Al6B-X where X = Li, Na, K or Mg). The alkali and alkaline earth ions, as well as boron-containing ions, are all naturally present in seawater (Li ≈ 0.020 mM, Na ≈ 480 mM, K ≈ 10 mM, Mg ≈ 55 mM, B ≈ 0.43 mM [26]). We evaluate the performance of the glasses using a combination of laboratory tests with barnacle larvae and adults, in comparison with field tests that evaluate the glasses in the marine environment. Also, we further explore the relationship between moulting and cement deposition using pressure cycle technology [27,28] to process cement collections and main body moults (exuviae), and investigate the effect of hydration on cement solubility.

2. Protein analysis of barnacle cement

We opted to extract proteins from hydrated cement plaques harvested from the underside of barnacles attached to silicone-coated panels and their exuviae, as we could collect enough material to fraction and process samples from the same barnacle using different solvents. We note that So *et al*. [9] found that cement protein profiles are mostly independent of substrate chemistry, and 89% of proteins identified in cement from barnacles attached to 2Al6B-Na are found in hydrated cement plaques of barnacles grown on silicone. HFIP enhanced the extraction of AaCP19 and AaCP43, whereas an aqueous urea buffer enhanced the extraction of AaCP52, AaCP57, AaCP100, as well as other non-structural proteins (figure 1; electronic supplementary material, tables S1 and S2); a more thorough examination of proteins extracted as a function of sample preparation is provided elsewhere [29]. Despite the link between moulting and cement deposition [15–17], with the exception of AaCP57, we detected little to no unique peptides from CPs in exuviae. These results suggest that the CPs, which have evolved an adhesive function, are enriched at the adhesive interface. Searches for sequence similarities between the AaCP57 family and the National Center for Biotechnology Information (NCBI) database using the Basic Logical Alignment Search Tool (BLAST) yielded no significant hits for homologous proteins. As was the case in our previous cement analysis [9], the CP20 homologues were not detected in significant amounts in the cement plaques or exuviae, However, we did detect AaCP20–2 in tissue collections that included the demineralized baseplate, cuticle and cement plaque (electronic supplementary material, table S3), which is consistent with the findings of He *et al*. [30] that AaCP20-2 is present in the basal shell. Kamino *et al*. [5] harvested cement from *M. rosa* by scraping the base of detached barnacles; therefore, the misclassification of CP20 as a cement protein is probably owing to the inclusion of baseplate particulate in their cement collections. We note that CP19, CP52, and CP100 are present in a transcriptome of a membranous barnacle (*Tetraclita japonica formosana*), whereas CP20 is absent [31], which further supports our position that CP20 is associated with the baseplate rather than the cement.

While our proteomics analysis provided insights into the protein profile at the adhesive interface, the mechanism by which the cement cures is unknown. Lysyl oxidase (AaLOx-1) and peroxidase (AaPx-2) were present in cement plaques and exuviae (figure 1), offering support to the hypothesis that cement polymerizes via mechanisms akin to wound healing [18]. However, one could also argue that

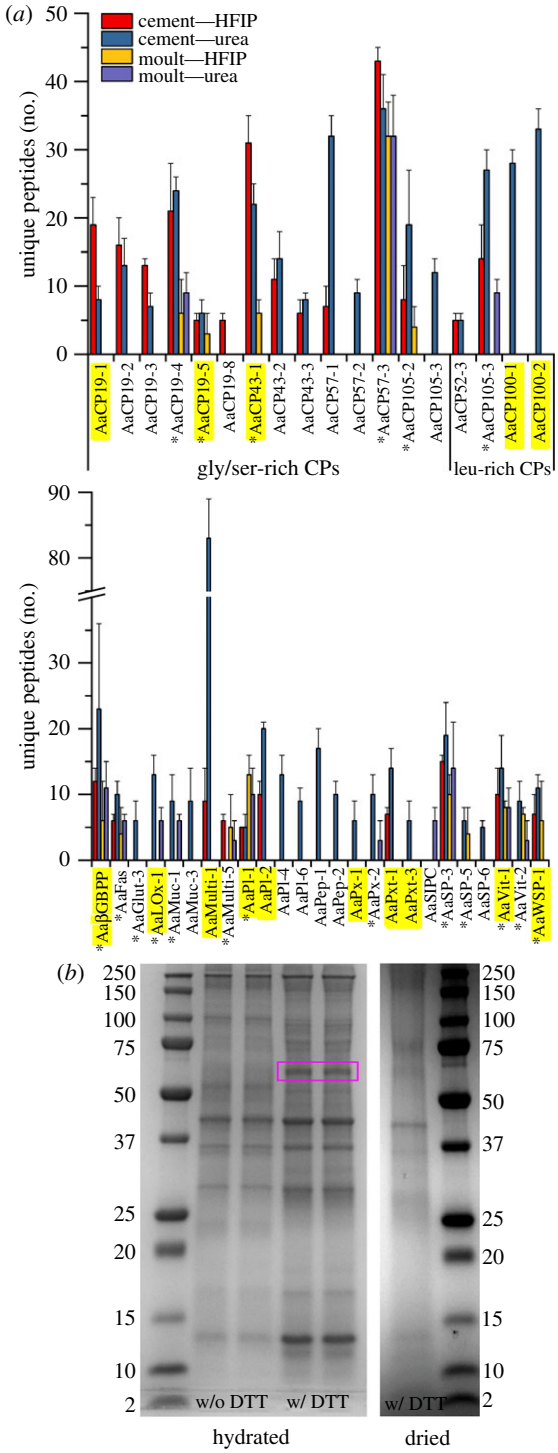

Figure 1. (*a*) Average number of unique peptides identified in hydrated cement plaques and body moults processed in HFIP or an aqueous urea buffer. Protein identifications in each sample were only accepted if a minimum of four unique peptides were detected at greater than 95% probability. Proteins shown were identified in three out of three cement plaques, at least five out of six moults in HFIP and at least four out of five moults in urea buffer. Asterisks denote proteins found in cement plaques and moults. Highlighted proteins were found in plaques of barnacles attached to 2Al6B-Na (minimum of four unique peptides) [9]. BGBPP, β-glucan-binding protein precursor; Fas, fasciclin; Glut, glutenin; Lox, lysyl oxidase; Muc, mucin; Multi, multifuncin; PI, protease inhibitor; Pep, peptidase; Px, peroxidase; Pxt, peroxinectin; SIPC, settlement-inducing protein complex; SP, serine protease; Vit, vitellogenin; WSP, waterborne settlement pheromone. (*b*) Sodium dodecyl sulfate–polyacrylamide gel electrophoresis (SDS–PAGE) gels of cement plaques collected from barnacles attached to 2Al6B-Na. Plaques were processes hydrated or pre-dried in Laemmli sample buffer with or without DTT.

they coincide in the body and the basal region to strengthen cuticular tissues rather than cross-link CPs. So *et al*. [9] found that the protein band at approximately 63 kDa is the most dominant band when proteins are extracted from cement plaques and cement attached to insoluble soda lime silicate (SLS) microspheres using HFIP; the band is not observed when using aqueous buffers [9,19]. Interestingly, we observed that the 63 kDa band was sufficiently solubilized when cement plaques from barnacles attached to 2Al6B-Na were heated in Laemmli sample buffer with 300 mM dithiothreitol (DTT) if the plaques remained hydrated prior to processing (figure 1). This observation suggests that the hydration state at the adhesive interface, and the possible complexation between proteins and glass degradation products, affects the solubility of the cement fibrils, which has implications with respect to barnacle adhesion on surface-active glasses.

3. Surface-active glasses

(a) Barnacle re-attachment assays

In re-attachment assays, we only used barnacles with translucent bases, i.e. no barnacles with opaque, hydrated cement deposits. Adult barnacles were transferred from silicone-coated panels and re-attached to surface-active glasses pre-soaked in artificial seawater (ASW) for at least 24 h. The pre-soak step was taken to avoid exposing barnacles to the high concentration of ions released during the initial rate-limited stage of glass dissolution before the formation of the diffusion-limiting reaction layer [22]. This step also minimized that pH increases during re-attachment assays, which were typically less than 0.1 and the maximum pH observed was 8.14; Nardone *et al*. [32] reported that barnacle adhesion is not heavily dependent on pH over the range of 7.50–8.01. Figure 2*a* shows that there was no statistical difference in the critical shear stress of barnacles that cleanly released from the glasses after 14 days. A portion of the barnacles re-attached to alkali aluminoborate glasses (approx. 20%) strongly adhered and their side shells fractured during push-off attempts. Conversely, no barnacles strongly adhered to 2Al6B-Mg. Push-off assays were performed within 5 min of removing the substrates from ASW to assess barnacle adhesion while the interface was hydrated. Once the gel layers fully dried, barnacles freely detached from glass substrates owing to adhesive failure between the reaction layer and unreacted glass, as cement fibrils did not pass through the reaction layer (figure 2*b*) despite its porosity (electronic supplementary material, figure S1). Because we did not observe any significant differences in the performance of the alkali aluminoborate glasses in push-off assays, we focused on the comparison of 2Al6B-Na to 2Al6B-Mg throughout the remainder of this study.

To discern whether released ions alone compromise adhesion or if adhesive failure between the reaction layer and the underlying glass also contributes, we substituted 5 mol % of the B_2O_3 in 2Al6B-Na and 2Al6B-Mg with SiO_2. We selected 5 mol % because this is the typical amount of SiO_2 contamination we detected in aluminoborate glasses melted in refractory crucibles suitable for large-scale production; all glasses in this study were melted in platinum crucibles to prevent any contamination. The addition of SiO_2 affects the glass reaction behaviour in two ways: (i) O–Si–O bonds are more resistant to hydrolytic degradation

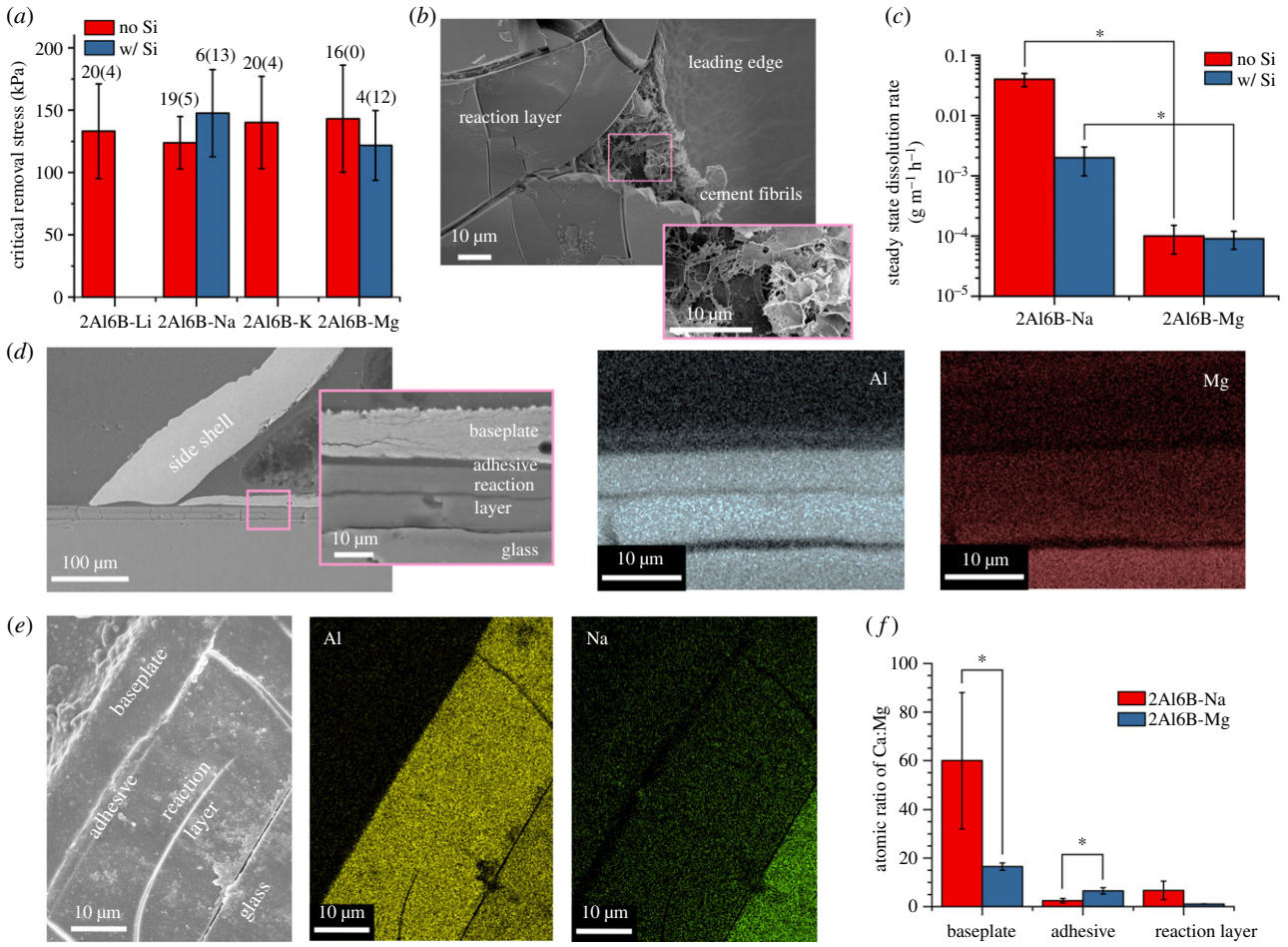

Figure 2. (*a*) Critical shear stress to remove *A. amphitrite* re-attached to aluminoborate glass plates for 14 days. Columns and error bars represent the means and standard deviations (s.d.). First number above the columns corresponds to the number of successfully detached barnacles; second (in parentheses) corresponds to the number of barnacles that broke during detachment. Force data for fractured barnacles were discarded. (*b*) scanning electron microscopy (SEM) images of the underside of *A. amphitrite* released from 2Al6B-Na after the substrate dried. (*c*) Steady-state dissolution rate of 2Al6B-Na and 2Al6B-Mg, with and without SiO_2 ($N = 3$; mean ± s.d.). SEM image and energy-dispersive spectroscopy (EDS) elemental maps from the cross-section of *A. amphitrite* on (*d*) 2Al6B-Mg and (*e*) 2Al6B-Na. (*f*) Atomic ratios of Ca : Mg of various regions in the cross-section, as determined by EDS point scans ($n = 3$; mean ± s.d.).

than O–B–O, increasing the chemical durability of the glass, and (ii) SiO_2 increases the dimensionality of the glass network, thereby providing covalent anchors between the reaction layer and the underlying glass [33]. While the critical removal stresses did not differ significantly for successful push-offs (figure 2*a*), the success rate dropped precipitously after the substitution of SiO_2 (figure 2*a*). The steady-state dissolution rate, i.e. the rate after a diffusion-limiting reaction layer forms [22], of 2Al6B-Na decreased by an order of magnitude with the addition of SiO_2 (figure 2*c*), which could account for some of the loss in performance. However, 2Al6B-Mg exhibited better performance at a slower dissolution rate than 2Al6B-Na with or without SiO_2. The disparity in dissolution rates suggests that Mg^{2+} ions disrupt adhesion processes more so than Na^+ ions, albeit the decrease in the push-off success rate with the addition of SiO_2 signifies that reaction layer properties also influence the foul-release performance.

To determine if ions released by the surface-active glass accumulate at the interface, barnacles re-attached to 2Al6B-Na and 2Al6B-Mg for 14 days were dehydrated in ethanol, then embedded in epoxy and cross-sectioned for scanning electron microscopy (SEM) analysis. Figure 2*d* shows that the leading edge of the barnacle was in intimate contact with the reaction layer on 2Al6B-Mg. Elemental maps of 2Al6B-Mg (figure 2*d*) and 2Al6B-Na (figure 2*e*) show an aluminium-rich reaction layer between the barnacle and the unreacted glass. In the case of 2Al6B-Mg, we also detected aluminium accumulating at the adhesive layer, which includes the cuticle (figure 2*d*). The depletion of magnesium and sodium in the reaction layers, as compared to the glasses, indicates that Mg^{2+} and Na^+ ions are being released to the surrounding environment.

The flux of Mg^{2+} ions at the interface is particularly important because increases in local Mg^{2+} concentrations inhibit calcite growth [34] and stabilize amorphous calcium carbonate in marine environments [35]. The atomic ratio of Ca : Mg at the adhesive interface of 2Al6B-Na, 2.5 ± 0.9 (figure 2*f*), is comparable to the ratio at the adhesive interface of barnacles grown on gold, 2.0 ± 1.0 [16]. In comparison to 2Al6B-Na, we observed an increase in calcium at the adhesive interface of 2Al6B-Mg, as noted by the twofold increase in the Ca : Mg ratio, and an increase in magnesium in the baseplate, as noted by the fourfold decrease in the Ca : Mg ratio. While the Ca : Mg ratio of the barnacle baseplate on 2Al6B-Mg (16.5 ± 1.5) is still greater than the required 4 : 1 ratio for the formation of calcite at 25°C [36], this ratio is near the lower limit for stable magnesium-substituted calcites (Ca : Mg = 14) [34]. If the local Ca : Mg ratio at the cuticle–baseplate interface, where nanocrystalline calcite is present

[37], enters the unstable calcite regime, the subsequent dissolution of calcite would account for the increase in calcium we observed at the adhesive interface. Hui *et al*. [38] demonstrated that the geometry and bending rigidity of the baseplate above the elastic cement layer influences barnacle adhesion via a crack-trapping mechanism. The higher success rate of barnacle removal on 2Al6B-Mg could be attributed to a lower bending rigidity of the baseplate, caused by calcite dissolution.

The physical properties of the reaction layers could also affect barnacle adhesion. Because the reaction layers on the surface-active glasses are analogous to compliant coatings on rigid substrates, barnacle adhesion could be dependent on the surface energy, elastic modulus and thickness of the reaction layers [39]. The reaction layers on 2Al6B-Na and 2Al6B-Mg predominantly consist of aluminium hydroxides; therefore, the surface energy of the reaction layers should be fairly equal. The dehydrated reaction layer on 2Al6B-Mg (approx. 15 µm; figure 2*d*) is nearly half the thickness of the layer on 2Al6B-Na (approx. 25 µm; figure 2*e*), and adhesion strength has been shown to decrease with increasing coating thickness [39]. However, the reduced modulus (electronic supplementary material, figure S2) of the reaction layer on 2Al6B-Na (27.0 ± 1.6 GPa) is nearly double the modulus of the layer on 2Al6B-Mg (15.2 ± 5.3 GPa), and adhesion strength has been shown to decrease with decreasing coating modulus [39]. The reaction layer modulus could also play a role in the poor performance of the SiO_2-containing glasses, as the addition of SiO_2 to 2Al6B-Na significantly increased the reduced modulus of the reaction layer (35.0 ± 3.4 GPa). We are unable to speculate to what extent these differences impact barnacle adhesion because the reaction layers were dehydrated; however, the results warrant future studies on the physical properties of these reaction layers, *in situ*, to determine if there is a correlation to barnacle adhesion.

(b) Larval toxicity and settlement assays

As Rittschof *et al*. demonstrated an excess of ions in seawater can affect larval behaviour and settlement [40], we performed toxicity assays using nauplii (first stage of larval development) and settlement assays using cyprids (last stage of larval development). Separate larvae were used for each experiment. Overall, we observed a low amount of nauplii deaths at the various glass surface area to ASW volume ratios (figure 3*a*); however, most nauplii were moribund and exhibited signs of intoxication (e.g. swimming in place, backwards or in circles) that typically precedes death by 48 h. Cyprids did not settle on the 2Al6B-Na or 2Al6B-Mg, and all cyprids were dead within 96 h. When cyprids were exposed to 2Al6B-Na for 24 h and then transferred to SLS tubes containing fresh ASW, there was no significant difference in settlement between cyprids exposed to 2Al6B-Na and the SLS control, although more cyprids died when exposed to 2Al6B-Na at the concentration of 0.2 cm^2 ml^{-1} (figure 3*b*). Cyprid settlement decreased by a factor of two with exposure to 2Al6B-Na for 48 h, but settlement was independent of the ratio of glass surface area to ASW volume. The mortality rate was higher after the longer exposure, but cyprids in nature would be unlikely to spend 48 h in close proximity to surface-active glasses. Instead, cyprids should be deterred from settling on surface-active glasses and move to other locations to settle.

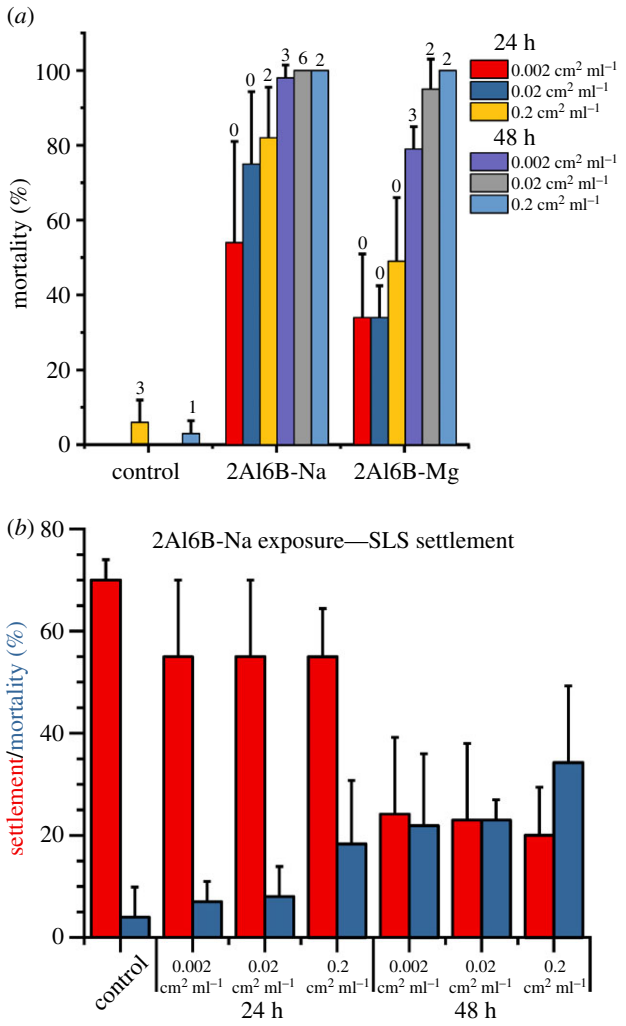

Figure 3. (*a*) Per cent of nauplii dead or moribund after exposure to various substrates for 24 and 48 h at different substrate surface areas to seawater volume ratios ($n = 3$; mean ± s.d.). Numbers above bars represent the number of dead nauplii. (*b*) Per cent of cyprids that settled or died in 24 h settlement assays that followed 24 or 48 h of exposure to 2Al6B-Na ($n = 5$; mean ± s.d.).

(c) Field tests

To assess the antifouling performance of 2Al6B-Na and 2Al6B-Mg glasses in natural marine environments, glass plates were mounted on high-density polyethylene panels and immersed at the Office of Naval Research (ONR) test facility at Port Canaveral, Florida for six months (23 February 2018 to 14 September 2018). Glass plates—along with inert (epoxy), foul-release (Intersleek® 900; IS900) and antifouling (BRA 640; BRA) controls—were held stationary in a vertical position in the water throughout the test period other than when they were removed from the water for monthly inspection. As shown in figure 4*a*, biofilms established themselves on all surfaces within the first month of immersion. While 2Al6B-Mg performed better than 2Al6B-Na for the first three months, macrofouler coverage increased over the last four months of immersion (in order of abundance; encrusting bryozoan > tubeworm > barnacle), and all panels were severely fouled (greater than 96% coverage) at the end of the immersion period (figure 4*b*).

Interestingly, multiple barnacle species—*A. amphitrite*, *Amphibalanus* (=*Balanus*) *eburneus*, *Amphibalanus* (=*Balanus*) *reticulatus* and *Amphibalanus* (=*Balanus*) *trigonus*—settled on the polyethylene panels to which the glass plates were

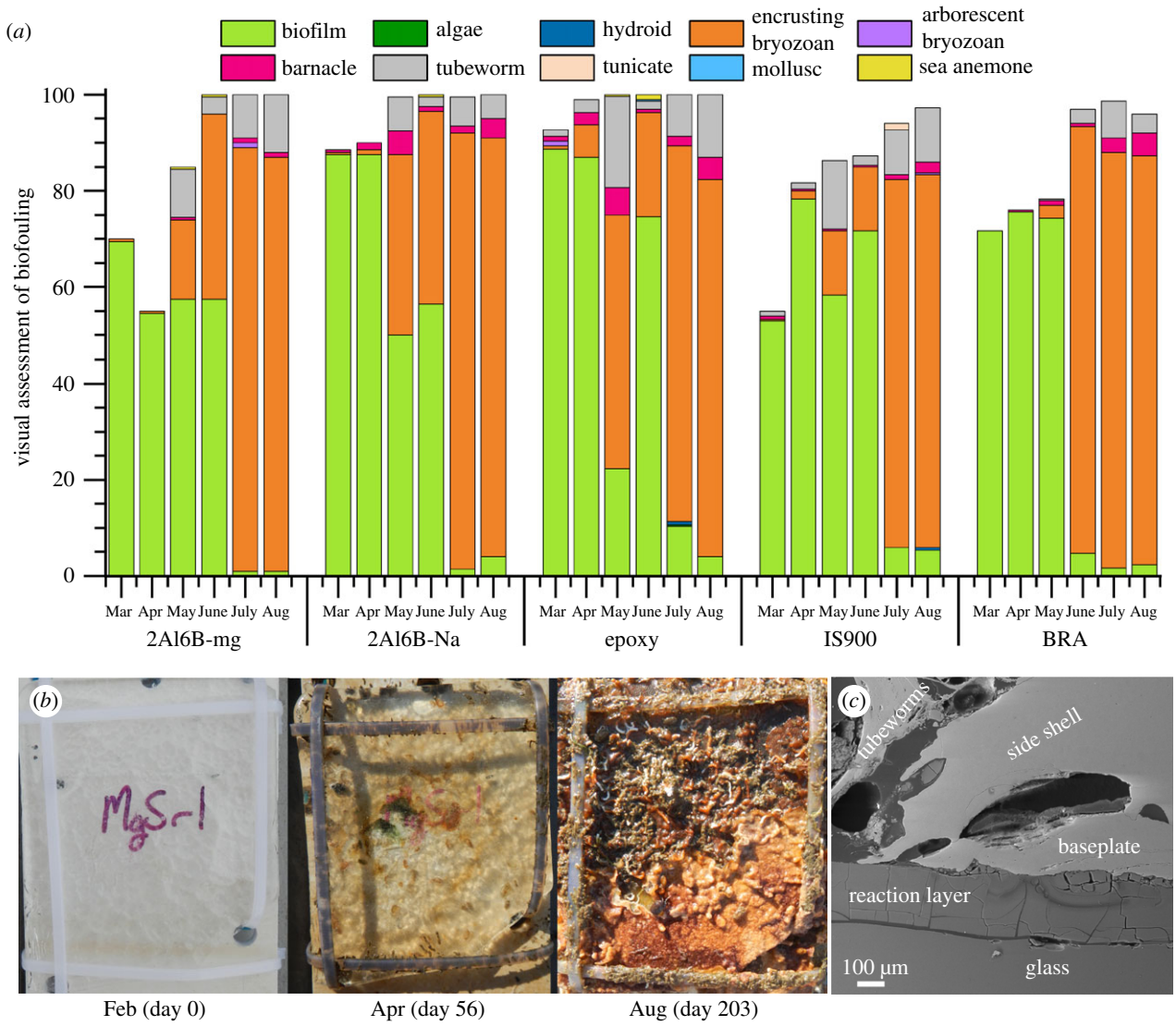

Figure 4. (*a*) Visual assessment of fouling coverage on surface-active glasses (2Al6B-Mg and 2Al6B-Na), an inert control (epoxy), a fouling-release control (IS900) and an antifouling control (BRA). Water quality and fouling community data are available in the electronic supplementary material, figure S2. (*b*) Photographs of fouling coverage on 2Al6B-Mg after 0, 56 and 203 days of immersion. (*c*) SEM image of the cross-section of *A. trigonus* settled on 2Al6B-Na.

mounted on; however, *A. trigonus* was the only species present on the surface-active glass panels. Therefore, *A. trigonus* cyprids could be more tolerant of the local environment at the glass–water interface. After the third month, push-off assays were attempted on barnacles settled on the glass panels, but barnacles were unable to be removed by a 20 lb force gauge. Despite the early establishment of a biofilm, figure 4*c* shows that *A. trigonus* is in intimate contact with the reaction layer, suggesting that *A. trigonus* also has a process to remove biofilms ahead of growth similar to *A. amphitrite* cyprids and barnacles [17,41,42]. We note the side shell and baseplate of *A. trigonus* (figure 4*c*) is considerably thicker than *A. amphitrite* (figure 2*d*), which could account for its resistance to fracture and displacement.

Because the formation of a thick biofilm probably diminishes the release of ions, we investigated the effect of periodic surface cleanings on the antifouling performance of 2Al6B-Mg. Panels were immersed for five months (3 August 2018 to 31 December 2018) and water jetted (120 psi) weekly, biweekly, monthly or not at all. Figure 5*a* shows that weekly water jetting did not prevent the establishment of a biofilm on 2Al6B-Mg or IS900; however, the biofilm coverage on 2Al6B-Mg was considerably lower than IS900 over the first three months. Similar to the first set of panels (figure 4*a*), during the third month, the presence of macrofouler communities substantially increased (tubeworm > barnacle > tunicate). Nevertheless, water jetting proved to be effective in reducing the macrofouler coverage, with coverage decreasing with increasing cleaning frequency (figure 5*b*).

4. Conclusion

These results show that increasing the interfacial concentration of ions that are naturally present in seawater is a viable approach to reducing macrofouler adhesion. This approach mitigates concerns over the bioaccumulation of the released compounds, as is the case with coatings that leach organometallic biocides. The heavy presence of macrofouling species on polyethylene panels, adjacent to surface-active glasses, indicates that organisms are unaffected by the release of ions if they are not in direct contact with the glass surface. Field tests confirm laboratory experiments that releasing Mg^{2+} ions is more effective at preventing macrofouler adhesion than releasing Na^{+} ions. However, neither 2Al6B-Mg nor 2Al6B-Na were effective at preventing the establishment of a biofilm even when cleaned weekly, albeit the cleaning protocols were mild and pressure washing

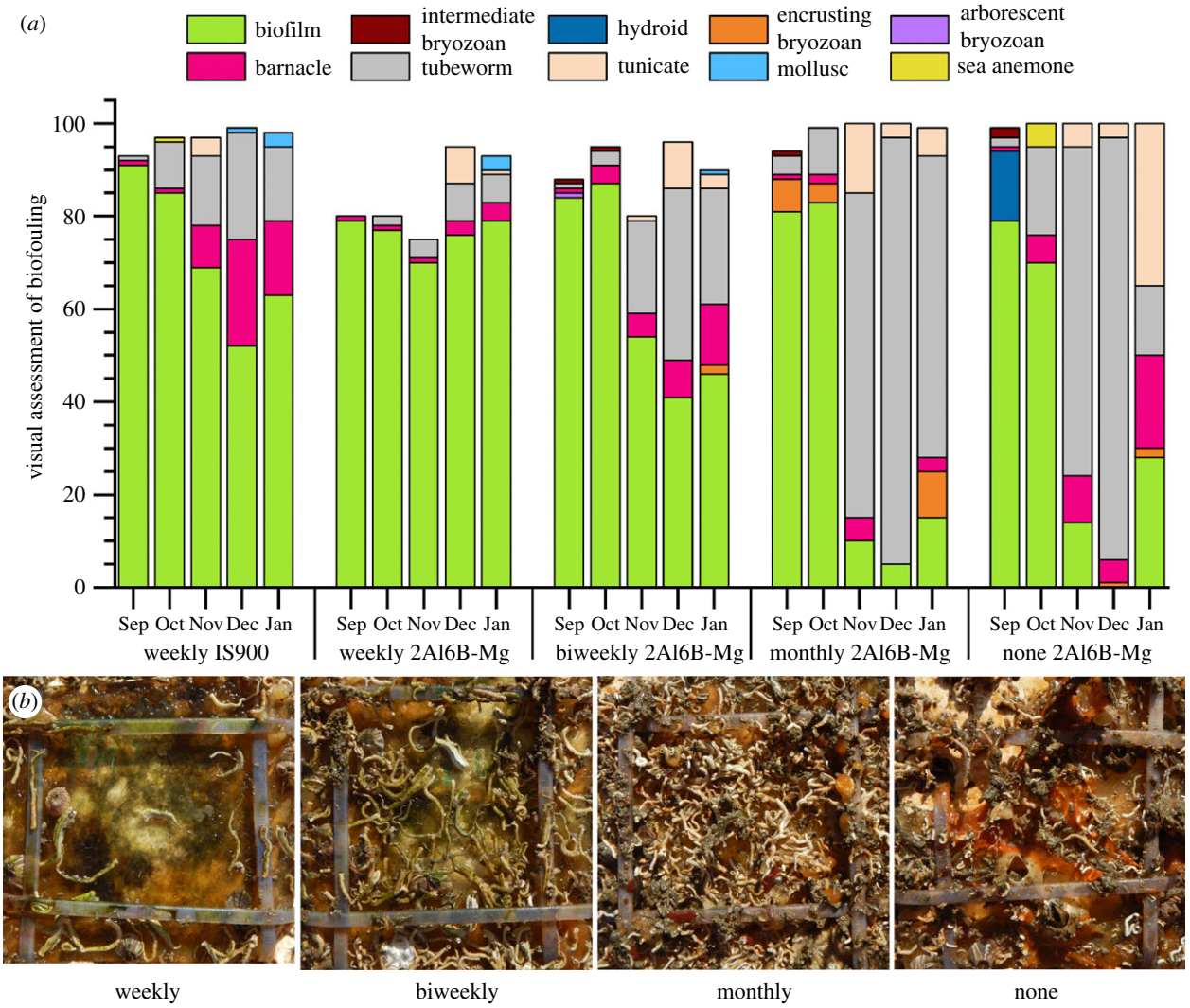

Figure 5. (*a*) Visual assessment of the fouling coverage on 2Al6B-Mg and IS900. Water jetting (120 psi) was performed at weekly, biweekly or monthly intervals. Water quality and fouling community data are available in the electronic supplementary material, figure S2, along with the complete dataset of the visual fouling assessments (electronic supplementary material, figures S4–S8). (*b*) Photographs of the fouling coverage on 2Al6B-Mg after 150 days of immersion. Panels were water jetted weekly, biweekly, monthly or not at all.

would probably be more effective at removing biofilms. While we focus on hard fouling in this study, the adhesion of biofilms is equally as important as they can promote the adhesion of some macrofouler communities [43]. In future studies, we will incorporate ions to challenge the formation of microbial biofilms to examine whether this increases the efficacy of the surface-active glasses for antifouling applications.

Ethics. This study was carried out in accordance with standard procedures for invertebrates.

Data accessibility. The mass spectrometry proteomics data have been deposited to the ProteomeXchange Consortium via the PRIDE partner repository with the dataset identifier PXD013036 and 10.6019/PXD013036.

Authors' contributions. K.P.F. was responsible for writing the manuscript, the conception and design of surface-active glasses and experiments involving said glasses, materials fabrication and characterization, and data analysis. A.B. performed materials fabrication and characterization, barnacle push-off assays, data analysis and assisting in writing duties under the supervision of K.P.F. A.W. and K.Z.H. managed field test experiments under the supervision of G.S. H.R. performed materials characterization under the supervision of K.J.W. J.N.S. performed proteomics experiments under the supervision of D.H.L. and C.M.S. B.O. reared larvae and barnacles for laboratory experiments and performed larval settlement and toxicity studies under the supervision of D.R. J.M.S. performed barnacle push-off assays. C.R.S. performed materials characterization.

Competing interests. We declare we have no competing interests.

Funding. This work was supported by the Office of Naval Research (ONR) through the basic research program at the Naval Research Laboratory (NRL) and by the ONR coatings program at NRL (N00014-16-1-3123), Duke Marine Laboratory (N00014-16-1-3112) and Florida Institute of Technology (N00014-16-1-3123). H.R. was supported through the American Society for Engineering Education post-doctoral fellowship program. J.N.S. was supported through the National Research Council post-doctoral fellowship program.

References

1. Yule AB, Walker G. 1987 Adhesion in barnacles. In *Barnacle biology* (ed. A Southward), pp. 389–402. Rotterdam, The Netherlands: A. A. Balkema.

2. Sullan RMA, Gunari N, Tanur AE, Chan Y, Dickinson GH, Orihuela B, Rittschof D, Walker GC. 2009 Nanoscale

structures and mechanics of barnacle cement. *Biofouling* **25**, 263–275. (doi:10.1080/08927010802688095)

3. Barlow DE, Dickinson GH, Orihuela B, Kulp III JL, Rittschof D, Wahl KJ. 2010 Characterization of the adhesive plaque of the barnacle *Balanus amphitrite*: amyloid-like nanofibrils are a major component. *Langmuir* **26**, 6549–6556. (doi:10.1021/la9041309)
4. Naldrett M, Kaplan D. 1997 Characterization of barnacle (*Balanus eburneus* and *B. cenatus*) adhesive proteins. *Mar. Biol.* **127**, 629–635. (doi:10.1007/s002270050053)
5. Kamino K, Odo S, Maruyama T. 1996 Cement proteins of the acorn barnacle, *Megabalanus rosa*. *Biol. Bull.* **190**, 403–409. (doi:10.2307/1543033)
6. Urushida Y, Nakano M, Matsuda S, Inoue N, Kanai S, Kitamura N, Nishino T, Kamino K. 2007 Identification and functional characterization of a novel barnacle cement protein. *FEBS J.* **274**, 4336–4346. (doi:10.1111/j.1742-4658.2007.05965.x)
7. Mori Y, Urushida Y, Nakano M, Uchiyama S, Kamino K. 2007 Calcite-specific coupling protein in barnacle underwater cement. *FEBS J.* **274**, 6436–6446. (doi:10.1111/j.1742-4658.2007.06161.x)
8. Kamino K. 2001 Novel barnacle underwater adhesive protein is a charged amino acid-rich protein constituted by a Cys-rich repetitive sequence. *Biochem. J.* **356**, 503–507. (doi:10.1042/bj3560503)
9. So CR *et al.* 2016 Sequence basis of barnacle cement nanostructure is defined by proteins with silk homology. *Sci. Rep.* **6**, 36219. (doi:10.1038/srep36219)
10. Nakano M, Kamino K. 2015 Amyloid-like conformation and interaction for the self-assembly in barnacle underwater cement. *Biochemistry* **54**, 826–835. (doi:10.1021/bi500965f)
11. Liang C, Li Y, Liu Z, Wu W, Hu B. 2015 Protein aggregation formed by recombinant cp19 k homologue of *Balanus albicostatus* combined with an 18 kDa N-terminus encoded by pET-32a (+) plasmid having adhesion strength comparable to several commercial glues. *PLoS ONE* **10**, e0136493. (doi:10.1371/journal.pone.0136493)
12. So CR, Liu J, Fears KP, Leary DH, Golden JP, Wahl KJ. 2015 Self-assembly of protein nanofibrils orchestrates calcite step movement through selective nonchiral interactions. *ACS Nano* **9**, 5782–5791. (doi:10.1021/acsnano.5b01870)
13. Wang Z *et al.* 2015 Molt-dependent transcriptomic analysis of cement proteins in the barnacle *Amphibalanus amphitrite*. *BMC Genom.* **16**, 859. (doi:10.1186/s12864-015-2076-1)
14. So CR, Yates EA, Estrella LA, Fears KP, Schenck AM, Yip CM, Wahl KJ. 2019 Molecular recognition of structures is key in the polymerization of patterned barnacle adhesive sequences. *ACS Nano* **13**, 5172–5183. (doi:10.1021/acsnano.8b09194)
15. Burden DK, Barlow DE, Spillmann CM, Orihuela B, Rittschof D, Everett R, Wahl KJ. 2012 Barnacle *Balanus amphitrite* adheres by a stepwise cementing process. *Langmuir* **28**, 13 364–13 372. (doi:10.1021/la301695m)
16. Burden DK, Spillmann CM, Everett RK, Barlow DE, Orihuela B, Deschamps JR, Fears KP, Rittschof D, Wahl KJ. 2014 Growth and development of the barnacle *Amphibalanus amphitrite*: time and spatially resolved structure and chemistry of the base plate. *Biofouling* **30**, 799–812. (doi:10.1080/08927014.2014.930736)
17. Fears KP, Orihuela B, Rittschof D, Wahl KJ. 2018 Acorn barnacles secrete phase-separating fluid to clear surfaces ahead of cement deposition. *Adv. Sci.* **5**, 1700762. (doi:10.1002/advs.201700762)
18. Dickinson GH, Vega IE, Wahl KJ, Orihuela B, Beyley V, Rodriguez EN, Everett RK, Bonaventura J, Rittschof D. 2009 Barnacle cement: a polymerization model based on evolutionary concepts. *J. Exp. Biol.* **212**, 3499–3510. (doi:10.1242/jeb.029884)
19. So CR *et al.* 2017 Oxidase activity of the barnacle adhesive interface involves peroxide-dependent catechol oxidase and lysyl oxidase enzymes. *ACS Appl. Mater. Interfaces* **9**, 11 493–11 505. (doi:10.1021/acsami.7b01185)
20. Sever MJ, Weisser JT, Monahan J, Srinivasan S, Wilker JJ. 2004 Metal-mediated cross-linking in the generation of a marine-mussel adhesive. *Angew. Chem.* **43**, 448–450. (doi:10.1002/anie.200352759)
21. Zhao H, Sun C, Stewart RJ, Waite JH. 2005 Cement proteins of the tube-building polychaete *Phragmatopoma californica*. *J. Biol. Chem.* **280**, 42 938–42 944. (doi:10.1074/jbc.M508457200)
22. Fears KP, Scancella JM, Orihuela B, Rittschof D, Wahl KJ. 2015 Surface-active borate glasses as antifouling materials. *Adv. Mater. Interfaces* **2**, 1500370. (doi:10.1002/admi.201500370)
23. Day DE, White JE, Brown RF, McMenamin KD. 2003 Transformation of borate glasses into biologically useful materials. *Glass Technol.* **44**, 75–81.
24. Hench LL. 2009 Genetic design of bioactive glass. *J. Eur. Ceram. Soc.* **29**, 1257–1265. (doi:10.1016/j.jeurceramsoc.2008.08.002)
25. Hench LL. 1998 Bioceramics. *J. Am. Ceram. Soc.* **81**, 1705–1728. (doi:10.1111/j.1151-2916.1998.tb02540.x)
26. Atkinson MJ, Bingman C. 1997 Elemental composition of commercial seasalts. *J. Aquaric. Aquat. Sci.* **8**, 39–43.
27. Tao F, Li C, Smejkal G, Lazarev A, Lawrence N, Schumacher RT. 2007 Pressure cycling technology (PCT) applications in extraction of biomolecules from challenging biological samples. *High Press Biosci. Biotech.* **1**, 166–173. (doi:11229/hpbb.1.166)
28. López-Ferrer D, Petritis K, Hixson KK, Heibeck TH, Moore RJ, Belov ME, Camp DG, Smith RD. 2008 Application of pressurized solvents for ultrafast trypsin hydrolysis in proteomics: proteomics on the fly. *J. Proteome Res.* **7**, 3276–3281. (doi:10.1021/pr7008077)
29. Schultzhaus JN, Dean SN, Leary DH, Hervey WJ, Fears KP, Wahl KJ, Spillmann CM. 2019 Pressure cycling technology for challenging proteomic sample processing: application to barnacle adhesive. *Integr. Biol.* **11**, 235–247. (doi:10.1093/intbio/zyz020)
30. He L-S, Zhang G, Qian P-Y. 2013 Characterization of two 20 kDa-cement protein (cp20 k) homologues in *Amphibalanus amphitrite*. *PLoS ONE* **8**, e64130. (doi:10.1371/journal.pone.0064130)
31. Lin H.-C., Wong YH, Tsang LM, Chu KH, Qian P-Y, Chan BK. 2014 First study on gene expression of cement proteins and potential adhesion-related genes of a membranous-based barnacle as revealed from next-generation sequencing technology. *Biofouling* **30**, 169–181. (doi:10.1080/08927014.2013.853051)
32. Nardone JA *et al.* 2018 Assessing the impacts of ocean acidification on adhesion and shell formation in the barnacle *Amphibalanus amphitrite*. *Front. Mar. Sci.* **5**, 369. (doi:10.3389/fmars.2018.00369)
33. Shelby JE. 2007 *Introduction to glass science and technology*. Cambridge, UK: Royal Society of Chemistry.
34. Berner R. 1975 The role of magnesium in the crystal growth of calcite and aragonite from sea water. *Geochim. Cosmochim. Acta* **39**, 489–504. (doi:10.1016/0016-7037(75)90102-7)
35. Raz S, Hamilton PC, Wilt FH, Weiner S, Addadi L. 2003 The transient phase of amorphous calcium carbonate in sea urchin larval spicules: the involvement of proteins and magnesium ions in its formation and stabilization. *Adv. Funct. Mater.* **13**, 480–486. (doi:10.1002/adfm.200304285)
36. Morse JW, Wang Q, Tsio MY. 1997 Influences of temperature and Mg : Ca ratio on $CaCO_3$ precipitates from seawater. *Geology* **25**, 85–87. (doi:10.1130/0091-7613(1997)025<0085:IOTAMC>2.3.CO;2)
37. De Gregorio BT, Stroud RM, Burden DK, Fears KP, Everett RK, Wahl KJ. 2015 Shell structure and growth in the base plate of the barnacle *Amphibalanus amphitrite*. *ACS Biomater. Sci. Eng.* **1**, 1085–1095. (doi:10.1021/acsbiomaterials.5b00191)
38. Hui C-Y, Long R, Wahl KJ, Everett RK. 2011 Barnacles resist removal by crack trapping. *J. R. Soc. Interface* **8**, 868–879. (doi:10.1098/rsif.2010.0567)
39. Rittschof D, Maki J, Mitchell R, Costlow JD. 1986 Ion and neuropharmacological studies of barnacle settlement. *J. Sea* **20**, 269–275. (doi:10.1016/0077-7579(86)90048-7)
40. Brady RF, Singer IL. 2000 Mechanical factors favoring release from fouling release coatings. *Biofouling* **15**, 73–81. (doi:10.1080/08927010009386299)
41. Gohad NV, Aldred N, Hartshorn CM, Lee YJ, Cicerone MT, Orihuela B, Clare AS, Rittschof D, Mount AS. 2014 Synergistic roles for lipids and proteins in the permanent adhesive of barnacle larvae. *Nat. Commun.* **5**, 4414. (doi:10.1038/ncomms5414)
42. Essock-Burns T, Gohad NV, Orihuela B, Mount AS, Spillmann CM, Wahl KJ, Rittschof D. 2017 Barnacle biology before, during and after settlement and metamorphosis: a study of the interface. *J. Exp. Biol.* **220**, 194–207. (doi:10.1242/jeb.145094)
43. Zardus JD, Nedved BT, Huang Y, Tran C, Hadfield MG. 2008 Microbial biofilms facilitate adhesion in biofouling invertebrates. *Biol. Bull.* **214**, 91–98. (doi:10.2307/25066663)